Supplementary Material

Sulfonated cobalt phthalocyanine/carbon nanotube hybrid as a bifunctional oxygen electrocatalyst

Chuan Li[a], Tianxiang Huang[a], Zhaodi Huang[b], Jianpeng Sun[b], Cheng Zong[a], Jingge Yang[a], Wenan Deng[a], Fangna Dai[b,*]

[a]The State Key Lab of Heavy Oil Processing, College of Chemical Engineering, China University of Petroleum (East China), Qingdao, Shandong 266580, PR China

[b]School of Materials Science and Engineering, College of Science, China University of Petroleum (East China), Qingdao, Shandong, 266580, PR China

*Corresponding authors: fndai@upc.edu.cn

The number of electrons involved in the ORR process was calculated using the Koutecky′–Levich (K-L) equation:

$$\frac{1}{j}=\frac{1}{j_l}+\frac{1}{j_k}=\frac{1}{B\omega^{1/2}}+\frac{1}{j_k}$$

$$B=0.62\,nFC_0{D_0}^{2/3}v^{-1/6}$$

$$j_k=nFkC_0$$

where, j is the measured current density, j_K and j_L are the kinetic and diffusion-limited current densities, respectively, ω is the angular frequency of the RDE in radians per second, n is the number of electrons involved in the reaction, F is the Faraday constant (96485 C mol^{-1}), D_0 is the diffusion coefficient of O_2 in the electrolyte (1.93×10^{-5} cm^2 s^{-1}), v is the kinematic viscosity of the electrolyte (1.01×10^{-2} cm^2 s^{-1}), C_0 is the concentration of O_2 in the electrolyte (1.26×10^{-6} mol cm^{-3}) and k is the electron transfer rate constant.

The electrochemically active surface area (ECSA) was determined by the double-layer capacitance (C_{dl}). To obtain the C_{dl} value, the capacitive current associated with double-layer in non-Faradaic region (1.10 to 1.20 V vs. RHE) was measured by cyclic voltammetry (CV) at different scan rates (20, 40, 60, 80 and 100 mV s^{-1}). A linear slope is obtained from the plot of the differences in the current density (J_a-J_c) at 1.15 V (vs. RHE) against the scan rate. The linear slope is equivalent to the twice of the C_{dl}.

the turnover frequency (TOF) values for OER were calculated from the equation as followed.

$$TOF = JA/4Fn$$

Where J is the current density at 1.63 V (vs. RHE), A is the surface area of the glassy carbon electrode, the number 4 means four electrons per mol of O_2, F represents the Faraday constant and n is the number of moles of the active sites on the electrode. In our work, we regard CoN4 species as the active sites, and do not consider the other moieties as active sites. According to the ICP-MS results and the catalyst loading amount on the glassy carbon electrode, the Co mass content can be obtained then the number of moles of CoN4 can be figured out. When calculating the TOF values, the molecular weights of Co, CoPc and CoPc-SO_3H are 58.93 g/mol, 571.46 g/mol and 811.64 g/mol respectively.

The probe tests were employed in oxygen-saturated 0.1 M KOH solution to investigate the role of cobalt in active site. HMTA (hexamethylenetetramine) is used as a coordination block of O_2 molecules to cobalt ions. Therefore, cobalt involvement in active site could be identified when comparing ORR behaviors with or without using HMTA.

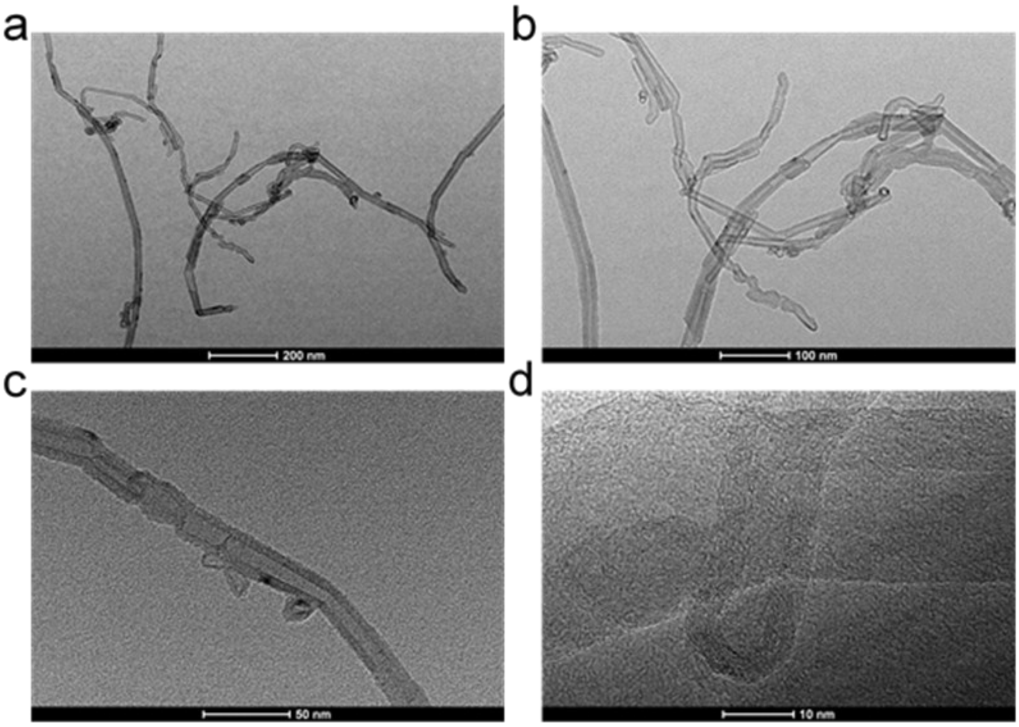

Fig. S1 HR-TEM images of CoPc–SO_3H/CNT hybrid in different scale bar. (a: 200 nm; b: 100 nm; c: 50 nm; d: 10 nm)

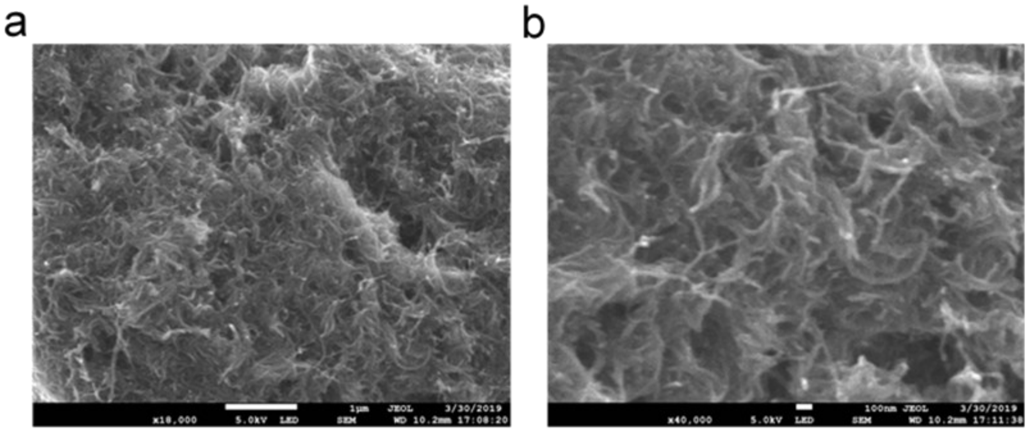

Fig. S2 SEM images of CoPc–SO_3H/CNT hybrid in different scale bar (a: 1 μm; b: 100 nm).

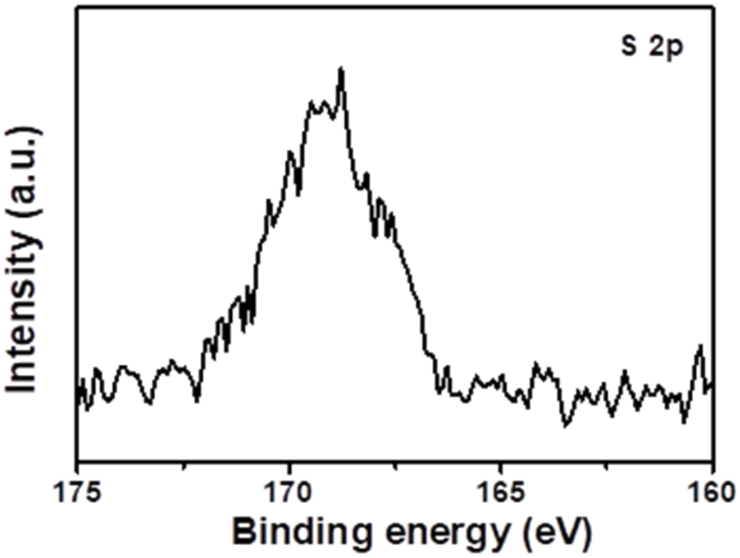

Fig. S3 XPS S 2p spectra of CoPc–SO_3H/CNT.

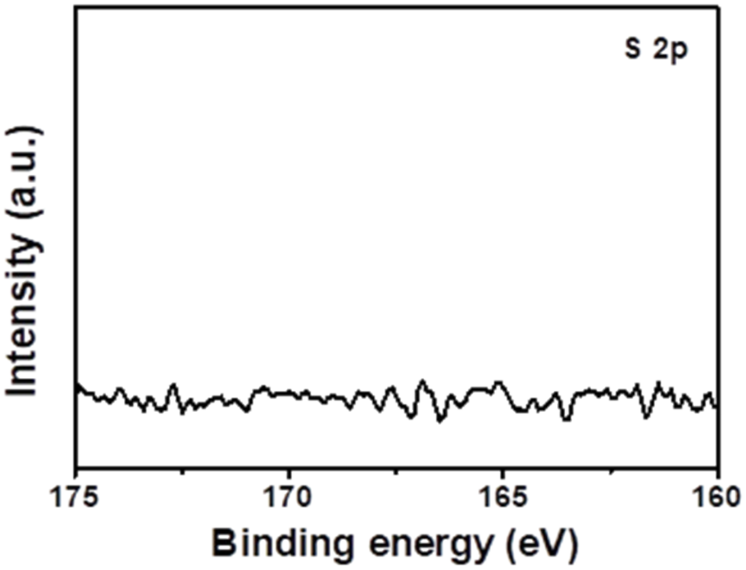

Fig. S4 XPS S 2p spectra of CoPc/CNT.

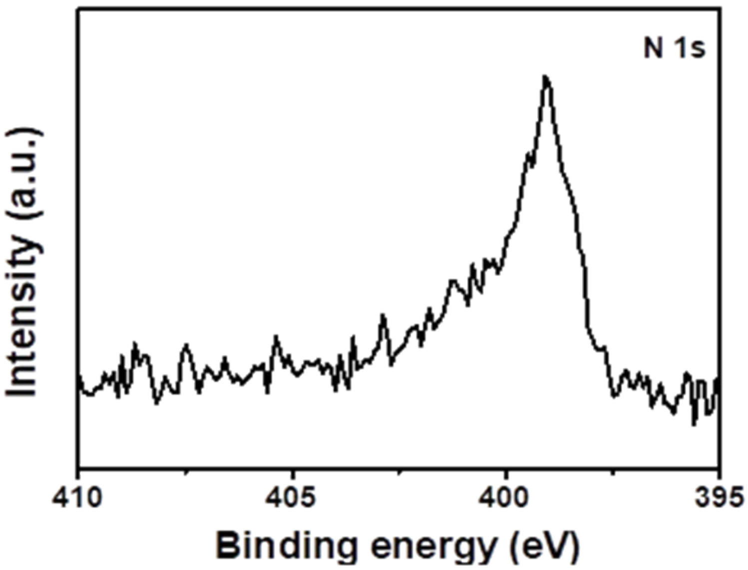

Fig. S5 XPS N 1s spectra of CoPc–SO_3H/CNT.

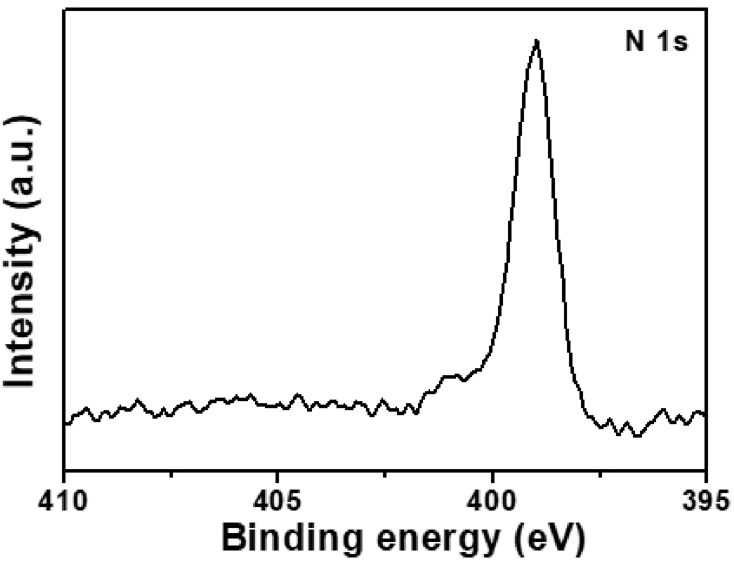

Fig. S6 XPS N 1s spectra of CoPc/CNT.

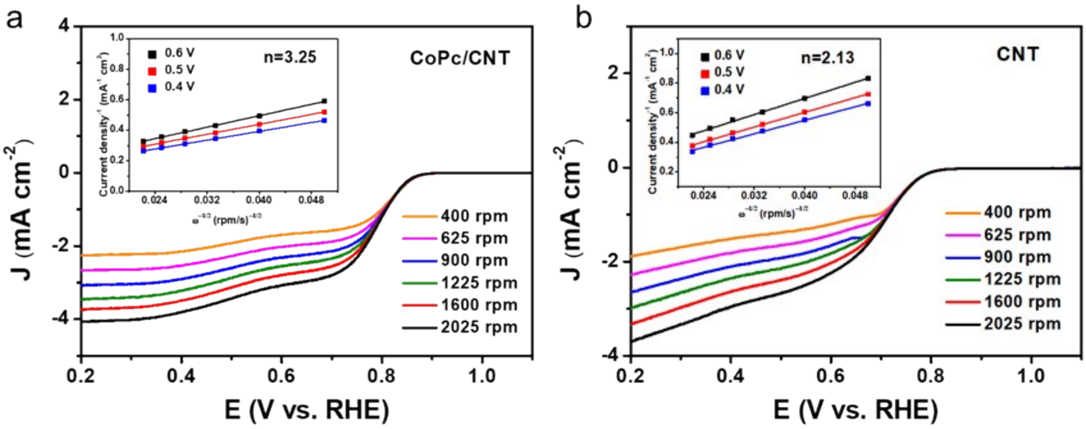

Fig. S7 LSV curves at various rotation rates of the (a) CoPc/CNT and (b) CNT in O_2-saturated 0.1 M KOH electrolyte with a sweep rate of 10 mV s^{-1}. (inset: corresponding K–L plots at various potentials).

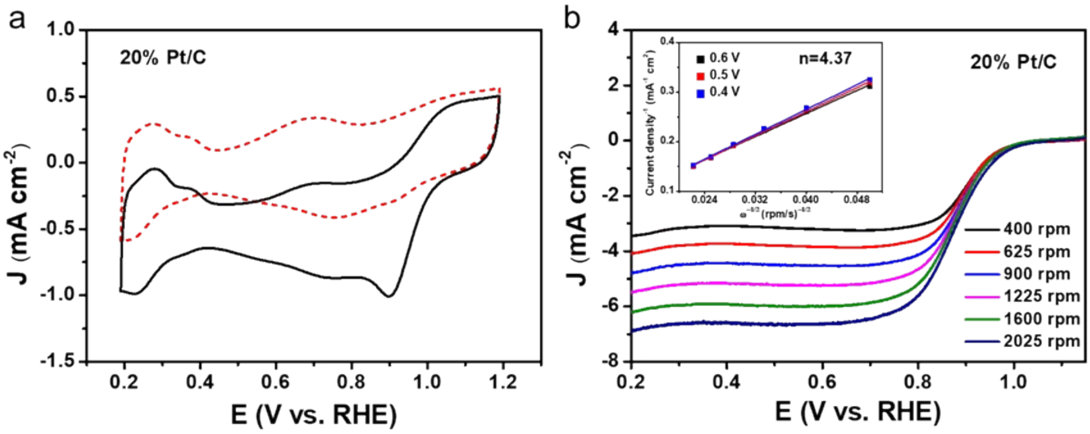

Fig. S8 (a) CVs of 20 wt% Pt/C in O_2-saturated (solid lines) and N_2-saturated (dotted line) 0.1 M KOH at 10 mV s^{-1}; (b) LSV curves at various rotating rates of 20 wt% Pt/C in O_2-saturated 0.1 M KOH electrolyte with a sweep rate of 10 mV s^{-1}. (inset: corresponding K–L plots at various potentials).

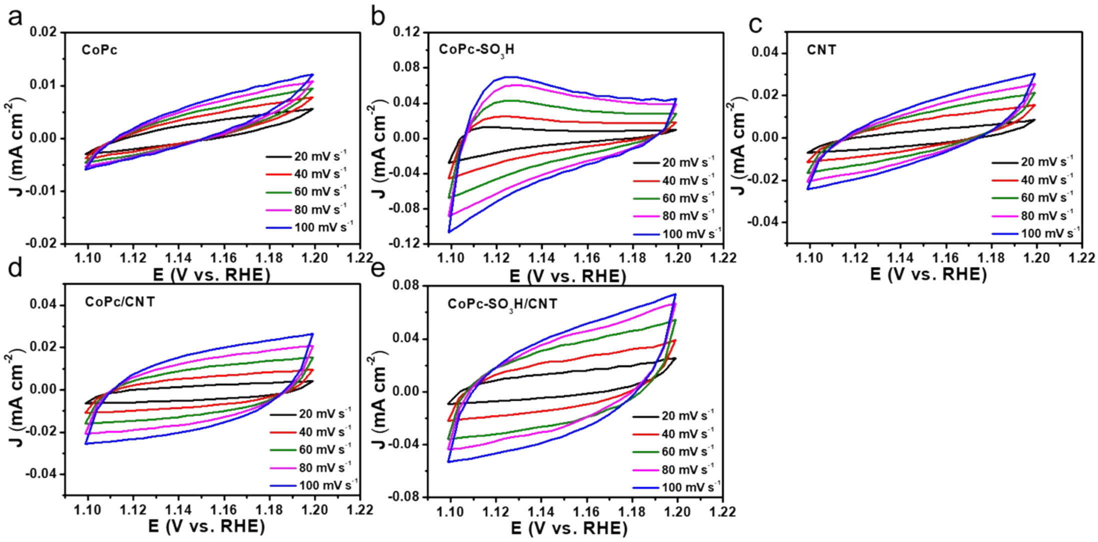

Fig. S9 CVs of (a) CoPc, (b) CoPc-SO$_3$H, (c) CNT and (d) CoPc/CNT and (e) CoPc-SO$_3$H/CNT in non-Faradaic region (1.10 to 1.20 V vs. RHE) at different scan rates from 20 to 100 mV s^{-1}.

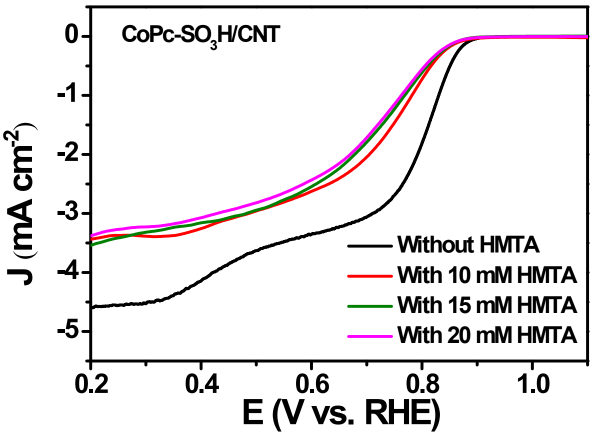

Figure S10. LSV curves of CoPc-SO_3H/CNT before and after probe tests at a rotation speed of 1600 rpm in oxygen-saturated 0.1 M KOH.

Table S1. The ORR performance of CoPc, CoPc-SO_3H, CNT, CoPc/CNT, CoPc-SO_3H/CNT and 20 wt% Pt/C in 0.1 M KOH at 1600 rpm.

Sample	**Onset potential E_0 (V)**	**Half wave potential $E_{1/2}$ (V)**	**Current density J_i (mA cm^{-2})**	**Tafel slope (mV dec^{-1})**	**Electron transfer number n**
CoPc	0.66	0.48	1.38	119	—
CoPc-SO_3H	0.77	0.63	2.39	74	—
CNT	0.80	0.66	3.34	66	2.13
CoPc/CNT	0.85	0.77	3.74	45	3.25
CoPc-SO_3H/CNT	0.88	0.78	4.60	41	3.99
20 wt% Pt/C	1.01	0.87	6.19	112	4.37

E_0: defined as the corresponding potential at -0.1 mA cm^{-2}.

J_i: defined as the corresponding current density at the potential of 0.2 V.

Table S2. The OER performance of CoPc, CoPc-SO_3H, CNT, CoPc/CNT and CoPc-SO_3H/CNT in 1 M KOH.

Sample	**Potential at 10 mA cm^{-2} (V)**	**Current density at 1.63 V (mA cm^{-2})**	**TOF value**	**Tafel slope (mV dec^{-1})**
CoPc	>2.00	0.02	0.0008	138
CoPc-SO_3H	1.64	5.20	0.3124	57
CNT	1.96	0.36	—	358
CoPc/CNT	1.74	0.31	0.0524	110
CoPc-SO_3H/CNT	1.62	14.86	11.373	48

Table S3. The OER performance of CoPc, CoPc-SO_3H, CNT, CoPc/CNT and CoPc-SO_3H/CNT in 0.1 M KOH.

Sample	**Potential at 10 mA cm^{-2} (V)**
CoPc	>2.00
CoPc-SO_3H	1.91
CNT	>2.00
CoPc/CNT	>2.00
CoPc-SO_3H/CNT	1.75

Table S4. Co loading amount detected by ICP-MS in CoPc/CNT, CoPc-SO_3H/CNT, CoPc-SO_3H/CNT(1:2), CoPc-SO_3H/CNT(1:1) and CoPc-SO_3H/CNT(2:1)

Sample	**Co loading amount (wt%)**
CoPc/CNT	2.58
CoPc-SO_3H/CNT	0.57
CoPc-SO_3H/CNT(1:2)	0.57
CoPc-SO_3H/CNT(1:1)	0.86
CoPc-SO_3H/CNT(2:1)	1.22

Table S5. Comparison study of some recently reported bi-functional ORR/OER catalysts in alkaline electrolyte.

Catalyst	**OER** $E_{j=10}$ **(V vs. RHE)**	**ORR** $E_{1/2}$ **(V vs. RHE)**	**ΔE** $(E_{j=10}-E_{1/2})$ **(V)**	**Electrolyte**	**Reference**
MCO@NCNTs	1.70	0.76*	0.94	0.1 M KOH	[1]
$CoFe_2O_4$/CNTs	1.65	0.75	0.90	0.1 M KOH	[2]
CoFe@NCNTs	1.68	0.84	0.84	0.1 M KOH	[3]
Co3O4/N-rGO	1.72	0.79	0.93	0.1 M KOH	[4]
$Co_{25}Zn_{75}$-C1000-5h	~1.80	~0.82	~0.98	0.1 M KOH	[5]
CoPc-SO_3H/CNT	1.75	0.78	0.97	0.1 M KOH	This work
$NiCo_2O_4$/Graphene	1.67	0.69	0.98	0.1 M KOH	[6]
Co_3O_4@PGC	1.72	0.69	1.03	0.1 M KOH	[7]

*:This value is ORR potential at -3 mA cm^{-2}.

Supplementary References

[1] Zhao T, Gadipelli S, He G, et al. Tunable Bifunctional Activity of MnxCo3− xO4 Nanocrystals Decorated on Carbon Nanotubes for Oxygen Electrocatalysis[J]. ChemSusChem, 2018, 11(8): 1295-1304.

[2] Zhang X, Xu H, Li X, et al. Facile synthesis of nickel–iron/nanocarbon hybrids as advanced electrocatalysts for efficient water splitting[J]. ACS Catalysis, 2015, 6(2): 580-588.

[3] Cai P, Hong Y, Ci S, et al. In situ integration of CoFe alloy nanoparticles with nitrogen-doped carbon nanotubes as advanced bifunctional cathode catalysts for Zn–air batteries[J]. Nanoscale, 2016, 8(48): 20048-20055.

[4] Li Y, Zhong C, Liu J, et al. Atomically Thin Mesoporous Co3O4 Layers Strongly Coupled with N-rGO Nanosheets as High-Performance Bifunctional Catalysts for 1D Knittable Zinc–Air Batteries[J]. Advanced Materials, 2018, 30(4): 1703657.

[5] Gadipelli S, Zhao T, Shevlin S A, et al. Switching effective oxygen reduction and evolution performance by controlled graphitization of a cobalt–nitrogen–carbon framework system[J]. Energy & Environmental Science, 2016, 9(5): 1661-1667.

[6] Lee D U, Kim B J, Chen Z. One-pot synthesis of a mesoporous $NiCo_2O_4$ nanoplatelet and graphene hybrid and its oxygen reduction and evolution activities as an efficient bi-functional electrocatalyst[J]. Journal of Materials Chemistry A, 2013, 1(15): 4754-4762.

[7] Li G, Wang X, Fu J, et al. Pomegranate-Inspired Design of Highly Active and Durable Bifunctional Electrocatalysts for Rechargeable Metal–Air Batteries[J].

Angewandte Chemie International Edition, 2016, 55(16): 4977-4982.